Journal of Alloys and Compounds 509S (2011) S804–S808

Contents lists available at ScienceDirect

Journal of Alloys and Compounds

journal homepage: www.elsevier.com/locate/jallcom

NMR study of metal-hydrogen systems for hydrogen storage

V.S. Kasperovich[a], M.G. Shelyapina[a,*], B. Khar'kov[a], I. Rykov[a], V. Osipov[a], E. Kurenkova[a], A.V. Ievlev[a], N.E. Skryabina[b], D. Fruchart[c], S. Miraglia[c], P. de Rango[c]

[a] Faculty of Physics, St Petersburg State University, 1 Ulyanovskaya St., Petrodvorets, 198504, St Petersburg, Russia
[b] Faculty of Physics, Perm State University, 15 Bukireva St., 614990, Perm, Russia
[c] Institut Néel, CNRS, BP 166, 38042 Grenoble Cedex 9, France

ARTICLE INFO

Article history:
Received 9 August 2010
Received in revised form 26 October 2010
Accepted 28 October 2010
Available online 10 November 2010

Keywords:
Hydrogen storage materials
Proton NMR
Spin-lattice relaxation

ABSTRACT

In this contribution we report on the results of our recent ^{1}H NMR studies of different metal hydrides of interest for reversible hydrogen storage applications: Ti–V–Cr alloys of various compositions, pure and with Zr_7Ni_{10} or Hf_7Ni_{10} additives, and in additives themselves. The temperature dependences of ^{1}H spin-lattice relaxation have been treated within an exchange model.

1. Introduction

During the last decades metal hydrogen systems as hydrogen storage materials were subject of intensive studies. Despite a considerable amount of both experimental and theoretical works, a fundamental and comprehensive understanding of intrinsic mechanisms that govern the thermodynamics and hydrogen kinetics in these hydrides still merits complementary investigations. In such perspectives, deeper knowledge on local structure and hydrogen mobility is helpfully required. Appreciable enlightening of main characteristics (static and dynamics) can be provided using nuclear magnetic resonance (NMR) method which is an especially powerful tool to investigate metal hydrogen systems [1–3].

The magnesium dihydride MgH_2 is one of the most attractive materials for hydrogen storage due to its high storage capacity (7.6 wt.% of hydrogen) and low cost of magnesium. However, its rather slow hydrogen absorption and desorption kinetics as well as high dissociation temperature, which is above 673 K, essentially limit its application for hydrogen storage. Numerous attempts have been made in order to improve magnesium hydrogen absorbing–desorbing characteristics. It has been reported experimentally that mixing magnesium or magnesium hydride with small amount of transition metals (TM) [4] or their oxides [5] essentially accelerates the hydrogen kinetics. However, the nature of this improvement up to now remains unclear.

Several attempts have been undertaken to explain it using NMR techniques. In Ref. [6] it has been found from ^{1}H NMR line width measurements that in coarse-grained MgH_2 the hydrogen hopping rate remains very slow up to 400 °C, whereas in MgH_2 ball-milled with Nb_2O_5 additives the fraction of mobile hydrogen grows continuously with temperature. That indicates the acceleration of reaction kinetics in this material is not only due to the decreased diffusion distance, caused by decreasing grain size, but also due to the faster hydrogen motion.

According to ^{1}H nuclear spin-lattice relaxation data in nano-scaled MgH_2 ball-milled with 10–15% V_2O_5 [7,8], the surface layer contains paramagnetic centres which are responsible for the spin-lattice relaxation rate enhancement. The authors suppose that these paramagnetic centres result from broken bonds on the surface of MgH_2 grains (these paramagnetic centres do not originate from the ball material) and could provide high catalytical activity of the mechanically activated Mg-based alloys.

NMR has been also applied to study hydrogen dynamics in magnesium–scandium hydrides. In Ref. [9] the rates of H and D atomic hopping in $MgScH_x$ metal-hydrides has been measured. In particular, it has been found that the motion of hydrogen in $MgScH_x$ is more rapid than in the metallic ScH_2 and the ionic MgH_2, but slower than in $LaNi_5H_x$. A new double-quantum NMR method with ^{45}Sc recouping reveals two types of deuterium with and without scandium neighbours [10], which indicates that a part of hydrogen

* Corresponding author at: Faculty of Physics, Department of Quantum Magnetic Phenomena, St Petersburg State University, 1 Ulyanovskaya St., Petrodvorets, 198504, St Petersburg, Russia. Tel.: +7 812 428 44 69; fax: +7 812 428 72 40.
E-mail address: marinashelyapina@mail.ru (M.G. Shelyapina).

0925-8388/$ – see front matter © 2010 Elsevier B.V. All rights reserved.
doi:10.1016/j.jallcom.2010.10.195

Table 1
Experimental structural data and calculated parameters of the exchange model of the proton spin-lattice relaxation for studied hydrides of $Ti_{0.33}V_{1.27}Cr_{1.4}$, $Ti_{0.5}V_{1.9}Cr_{0.6}$, $TiV_{0.8}Cr_{1.2}H_{5.29}$, $TiV_{0.8}Cr_{1.2}$ + 4 at.%Zr_7Ni_{10} and $TiV_{0.8}Cr_{1.2}$ + 4 at.%Hf_7Ni_{10} alloys; the values of τ_0 and $\tau_c^{300\,K}$ are given for the mobile/bounded hydrogen states.

Parameters		$Ti_{0.33}V_{1.27}Cr_{1.4}$	$Ti_{0.5}V_{1.9}Cr_{0.6}$	$TiV_{0.8}Cr_{1.2}$	$TiV_{0.8}Cr_{1.2}$ + 4 at.%Zr_7Ni_{10}	$TiV_{0.8}Cr_{1.2}$ + 4 at.%Hf_7Ni_{10}
Structure type	Alloy	bcc	bcc	bcc	bcc[a]	bcc[a]
	Hydride	bcc	fcc	fcc	fcc[a]	fcc[a]
Lattice parameter	Alloy	2.981 ± 0.002	3.028 ± 0.002	3.046 ± 0.002	3.026 ± 0.002[a]	3.041 ± 0.002[a]
	Hydride	3.036 ± 0.002	4.269 ± 0.002	4.282 ± 0.002	4.255 ± 0.004[a]	4.271 ± 0.004[a]
p_m/p_b		0.35/0.65	0.45/0.55	0.30/0.70	0.37/0.63	0.36/0.64
E_a (kJ/mol)		10.6	10.7	12.4	13.0	12.9
$\tau_0(\times 10^{-11}$ s)		3.1/420	2.4/650	2.2/520	2.2/520	2.0/550
$\tau_c^{300\,K}(\times 10^{-9}$ s)		2.2/294	1.7/474	3.2/746	3.3/759	3.5/970
$S_2(G^2)$		35	38	28	26	20
K (Ks)		53	53	53	30	33

[a] Structure type and lattice parameter are given for the main phase ($TiV_{0.8}Cr_{1.2}$).

atoms are more mobile than the rest. Moreover, NMR measurements confirm a non-statistical Mg and Sc distribution over the crystal lattice.

The Ti–V–Cr alloys belong to a class of body centred cubic systems and exhibit potentially excellent characteristics of hydrogen storage properties with maximum uptake of more than 3.5 wt.% hydrogen for the most appropriate compositions. According to the ternary phase diagram, Ti–V–Cr alloys crystallize mostly to bcc structure, except narrow region near $TiCr_2$ composition with Laves phase AB_2 structure, which forms extremely stable hydride. However, even small amounts of V promote the bcc phase formation. In the bcc structure, Cr is the element that moderates the thermal stability of the hydride. Due to the bigger covalent radius (compared to Cr and V atom), with the Ti content increasing, the lattice parameter of the bcc alloy increases. It reaches a maximum for 33.33 at.% of Ti and the atomic percentage ratio Cr/V equal to 1.5 (formula $TiV_{0.8}Cr_{1.2}$) and decrease for lower or higher ratio. Increasing the lattice parameter leads to increasing the interstitial space and likewise the number of available hydrogen sites. The stability of these sites also changes with the composition of the alloy [11].

Besides the better thermodynamic properties, these ternary alloys exhibit rather fast hydrogen sorption kinetics (compared to MgH_2) which can be improved further by alloying with Zr_7Ni_{10} or Hf_7Ni_{10} [12]. Despite numerous NMR studies of hydrides of pure Ti, V, Cr and binary Ti–V, V–Cr alloys, the ternary Ti–V–Cr systems which is interesting in terms of hydrogen storage have not been investigated by NMR before to our knowledge.

In this paper, we report on the results of our ^{1}H NMR study of hydrogen mobility in ternary Ti–V–Cr alloys of various compositions ($TiV_{0.8}Cr_{1.2}$ as a basic composition, $Ti_{0.33}V_{1.27}Cr_{1.4}$ as a Cr rich compound, and $Ti_{0.5}V_{1.9}Cr_{0.6}$ as a vanadium rich compound), $TiV_{0.8}Cr_{1.2}$ with Zr_7Ni_{10} or Hf_7Ni_{10} additives, and in additives themselves.

2. Sample preparation and experimental methods

$TiV_{0.8}Cr_{1.2}$, $Ti_{0.33}V_{1.27}Cr_{1.4}$, $Ti_{0.5}V_{1.9}Cr_{0.6}$, Zr_7Ni_{10} and Hf_7Ni_{10} samples have been prepared by induction melting of the pure elements (Treibacher Industries AG) in argon atmosphere and melted three times each. The button-type ingot obtained was about 20 g in mass. A part of each sample, obtained after melting, was hand-crushed into fine powder (200 μm), for XRD analysis, using a steel mortar in the air atmosphere.

Another part of each sample was hydrogenated in autoclave at pressure 20 bar and temperature 200 °C. The estimation of the quantities of hydrogen absorbed by the samples was made by weighting the samples before and after their hydrogenation. That resulted in the formulas $TiV_{0.8}Cr_{1.2}H_{5.29}$, $Ti_{0.33}V_{1.27}Cr_{1.4}H_{1.13}$, $Ti_{0.5}V_{1.9}Cr_{0.6}H_{5.03}$, $Zr_7Ni_{10}H_{16.76}$ and $Hf_7Ni_{10}H_{8.03}$. The grain size after hydrogenation was less than 100 μm. That is comparable to radiofrequency skin thickness in such materials.

To prepare samples with additives $TiV_{0.8}Cr_{1.2}$ has been remelted with 4 at.% of Zr_7Ni_{10} or Hf_7Ni_{10}, after that they were hydrogenated using the same techniques as it is described above.

The structural characterizations of the samples before and after hydrogenation were done using a Siemens D-5000 X-ray diffractometer operated at Co Kα radiation at room temperature. The structure type and lattice parameters for Ti–V–Cr alloys before and after their hydrogenation are listed in Table 1. It is worth noting that all compounds except Zr_7Ni_{10} remains crystalline after hydrogenation, whereas Zr_7Ni_{10} becomes partly amorphous that is in agreement with results of structural study made in Ref. [13].

The pulse ^{1}H NMR spectra were recorded within the temperature range from 180 to 380 K on home-built NMR spectrometer at 20 MHz. The temperature range was restricted by the low hydrogen release temperature of studied alloys. The temperature of the samples was controlled with the accuracy ±0.5 K. The spin-lattice relaxation times T_1 were measured using the inversion recovery techniques.

The line shapes of the samples were also tested with home-built cw NMR spectrometer (42 MHz). During the cw NMR experiment the first derivative of the absorption spectral line was recorded. However, in Fig. 1 we show the ^{1}H NMR spectrum in $TiV_{0.8}Cr_{1.2}H_{5.29}$ hydride in more usual view, after integration of the experimental signals. The ^{1}H spectra in $Ti_{0.33}V_{1.27}Cr_{1.4}H_{1.13}$ and $Ti_{0.5}V_{1.9}Cr_{0.6}H_{5.03}$ are similar to the spectrum in Fig. 1. It is worth noting, that cw NMR spectra are always distorted due to the finite amplitude of the modulation field A_m. The effect is important if the line width is comparable to the A_m value. In our case, all spectra were treated using the home-built program, which takes into account the modulation effect and provides real line intensities and widths.

As it is evident from Fig. 1, the ^{1}H NMR spectrum of studied metallic hydrides consist of two lines: narrow and broad, shifted one relative to another, that corresponds to the hydrogen existing in two states: mobile (m) and bounded to the lattice (b), respectively. And one can suppose that there is an exchange between these two states. To treat the temperature dependences of ^{1}H T_1 in Ti–V–Cr hydrides we applied the modified Bloembergen–Purcell–Pound (BPP) model [14] assuming a fast exchange between mobile and bounded to the lattice hydrogen states [15]. This model can be applied in a case when the life time of hydrogen in these states (τ_m,τ_b) is much less the spin-lattice relaxation time $\tau_{m,b} << T_1$ and the relaxation functions can be described by an average exponential function:

$$F_1(t) = \exp\left(-t\left(\frac{p_m}{T_{1,m}} + \frac{p_b}{T_{1,b}}\right)\right), \quad (1)$$

where p_m and p_b are relative concentrations of hydrogen in mobile and bounded states ($p_m + p_b = 1$).

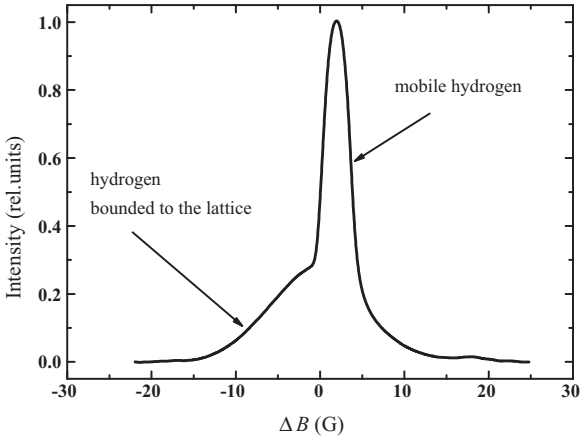

Fig. 1. ^{1}H NMR spectrum in $TiV_{0.8}Cr_{1.2}H_{5.29}$ at 42 MHz at room temperature. The spectrum is superposition of broad and narrow components.

In all studied Ti–V–Cr hydrides magnetization recovery curves were described by a single exponential decay (see Section 3.1), i.e. the spin-lattice relaxation times for both hydrogen magnetizations are equal. That means that the exchange between these two states is fast in comparison to the spin-lattice relaxation rate and for T_1 on can applied Eq. (1). It is worth noting that the presence of two lines in ^{1}H NMR spectra also points out that for the proton spin–spin relaxation one deals with either slow or intermediate exchange.

For the systems where ^{1}H–^{1}H dipole interactions dominates, to decrease the number of fitting parameters we can neglect the contributions of dipole interactions of protons with metal nuclei (see Ref. [15]), the only contributions taken into account were from ^{1}H–^{1}H dipole interactions and from conduction electrons:

$$T_1^{-1} = T_{1HH}^{-1} + T_{1e}^{-1} \quad (2)$$

where

$$T_{1HH}^{-1} = \frac{2}{3}\left(p_m S_{2HH}\left(\frac{\tau_{cm}}{1+\omega_0^2\tau_{cm}^2} + \frac{4\tau_{cm}}{1+4\omega_0^2\tau_{cm}^2}\right) + p_b S_{2HH}\left(\frac{\tau_{cb}}{1+\omega_0^2\tau_{cb}^2} + \frac{4\tau_{cb}}{1+4\omega_0^2\tau_{cb}^2}\right)\right), \quad (3)$$

S_{2HH} is the second moment due to ^{1}H–^{1}H dipole interactions, $\tau_{cm,b}$ is the correlation time that characterizes magnetic field fluctuation on the mobile and bounded to the lattice ^{1}H nuclei, ω_0 is the ^{1}H resonance frequency. The conduction electron contribution can be estimated from the relation $K = T_{1e}T$ with Korringa constant $K = 53 \pm 9$ Ks [15].

The temperature dependence of relaxation times is mainly defined by the correlation time, which is usually written within the activation model $\tau_c = \tau_0 e^{E_a/RT}$, where E_a is the activation energy of hydrogen motion, R is the gas constant, τ_0 is a pre-exponential factor. The second moment S_2 was calculated using the well-known van Vleck expression. For more details see Ref. [15].

3. Results and discussion

3.1. Ti–V–Cr hydrides

The magnetization recovery curves for the spin-lattice relaxation times of ^{1}H in $Ti_{0.5}V_{1.9}Cr_{0.6}H_{5.03}$, $Ti_{0.33}V_{1.27}Cr_{1.4}H_{1.13}$, $TiV_{0.8}Cr_{1.2}H_{5.29}$ were described by a single exponential decay over all temperature. The proton T_1 values of the three samples measured at 20 MHz are plotted as a function of inverse temperature in Fig. 2. It is clearly seen that the ^{1}H T_1 strongly depends on the composition of the Ti–V–Cr alloy. As a fraction of vanadium in the alloy increases, the minimum of T_1 shift towards the low-temperature side. This tendency is similar to that obtained for binary Ti–V alloys reported in Ref. [16]. The T_1 minimum values are higher for the alloys having the lower concentrations of vanadium: 11, 15, and 19 ms for $Ti_{0.5}V_{1.9}Cr_{0.6}H_{5.03}$, $Ti_{0.33}V_{1.27}Cr_{1.4}H_{1.13}$, and $TiV_{0.8}Cr_{1.2}H_{5.29}$, respectively. This is close to the values, obtained in binary Ti–V alloys. However, the minima are shifted towards the high temperature. In the high-temperature range ($\omega_0\tau << 1$) the T_1 values of the different samples do not agree with each other, moreover, the T_1 versus $1/T$ profile strongly depends on the composition. As the fraction of vanadium decreases, the radius of the curvature in the T_1 versus $1/T$ plot becomes short, as it is seen in Fig. 2.

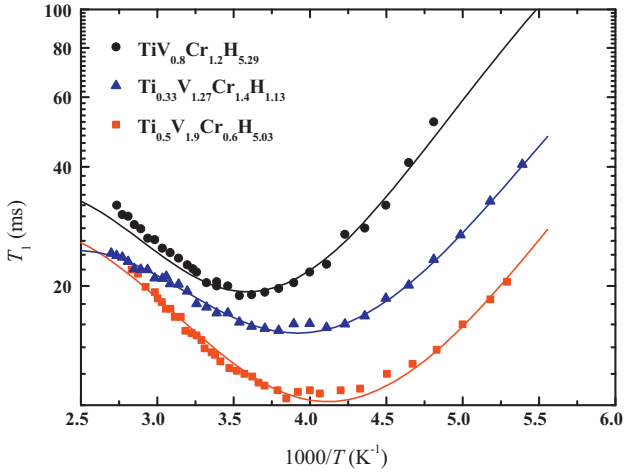

Fig. 2. Proton spin-lattice relaxation time T_1 at 20 MHz in $Ti_{0.5}V_{1.9}Cr_{0.6}H_{5.03}$, $Ti_{0.33}V_{1.27}Cr_{1.4}H_{1.13}$ and $TiV_{0.8}Cr_{1.2}H_{5.29}$ as a function of inverse temperature. The lines correspond to the fitting using exchange model.

To estimate the parameters of the hydrogen mobility in these samples the experimental data have been fitted within the exchange model briefly described in Section 2. To estimate the contribution of ^{1}H–^{51}V dipole interaction to proton relaxation in $TiV_{0.8}Cr_{1.2}H_{5.29}$ we calculated the second moment S_2 using the well-known van Vleck equation and supposing equiprobable distribution of the V atoms on the metal sites in lattice and H atoms on the tetrahedral interstitial sites. It was obtained, that vanadium contribution is less than 20% and was neglected.

To test the presence of paramagnetic atoms in the samples, the ^{1}H NMR spectra at 42 and 24 MHz have been recorded. It has been obtained that the second moment S_2 of the broad component depends on neither magnetic field nor temperature. That means the V and Cr atoms are not paramagnetic in these compounds. This has been also confirmed by the magnetic susceptibility measurements.

The application of the exchange model provides very promising results in description of both temperature and frequency dependences of the ^{1}H T_1 in $TiV_{0.8}Cr_{1.2}H_{5.29}$. It also results in a fair agreement between theoretical (28 G^2) and experimental (30 ± 1 G^2) values of the second moment S_2 that cannot be obtained within classical BPP model even taking into account the activation energy (and/or correlation time) distribution [15]. Applying the exchange model we suppose that the activation energy, which is mostly determined by nearest neighbour metallic atoms, is the same for mobile and bounded hydrogen, whereas the correlation time (life time in one state or another), which also depends on the number of vacant tetrahedral sites in the nearest neighbouring of the mobile hydrogen atom, is different.

The other two hydrides, bcc-$Ti_{0.33}V_{1.27}Cr_{1.4}H_{1.13}$ and fcc-$Ti_{0.5}V_{1.9}Cr_{0.6}H_{5.03}$, compared to $TiV_{0.8}Cr_{1.2}H_{5.29}$, contain less hydrogen or more vanadium, respectively. In order to estimate contribution ^{1}H–^{51}V dipole interactions to proton spin-lattice relaxation leads to 4% for $Ti_{0.33}V_{1.27}Cr_{1.4}H_{1.13}$ and 38% for $Ti_{0.5}V_{1.9}Cr_{0.6}H_{5.03}$, respectively. That means that despite the rather small hydrogen content in bcc-$Ti_{0.33}V_{1.27}Cr_{1.4}H_{1.13}$, the ^{1}H–^{1}H dipole interactions dominate and the model can be applied. For fcc-$Ti_{0.5}V_{1.9}Cr_{0.6}H_{5.03}$ the situation is different, although the hydride contains high amount of hydrogen and almost all tetrahedral interstitial sites are occupied, the ^{1}H–^{51}V dipole interactions are not negligible. To take it into account, and at the same time not to increase the number of fitting parameters of the model, we use in Eq. (3) the full second moment due to both ^{1}H–^{1}H and ^{1}H–^{51}V dipole interactions. This kind of approach is a rather typical for such systems. For example, in hydrides of binary Ti–V alloys to explain the proton spin-lattice relaxation the contribution of vanadium was artificially understated (see Ref. [17] and references therein).

As it is clearly seen in Fig. 2, the applied model almost perfectly fits the experimental temperature dependences for all compounds. The parameters of the model are listed in Table 1. The activation energy decreases with the vanadium concentration increasing, that results to the shift of the T_1 minimum towards low temperatures. The pre-exponential factor τ_0 for the bounded hydrogen seems to be more sensitive to the titanium content: it decreases with Ti concentration decreasing. As for the pre-exponential factor τ_0 for the mobile hydrogen, it does not change noticeably, but its smallest value corresponds to the fcc-$Ti_{0.5}V_{1.9}Cr_{0.6}H_{5.03}$ hydride with the lowest content of chromium. Summarising the data listed in Table 1, the activation process starts earlier for

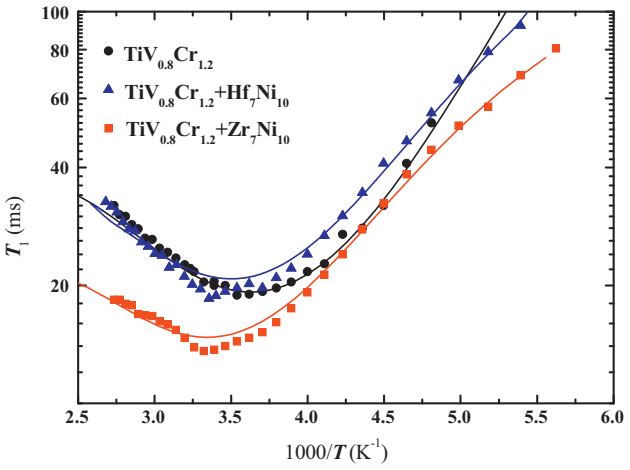

Fig. 3. Proton spin-lattice relaxation time T_1 at 20 MHz as a function of inverse temperature in hydrides of pure $TiV_{0.8}Cr_{1.2}$ and with 4 at.% of Zr_7Ni_{10} or Hf_7Ni_{10} additives. The lines correspond to the fitting using exchange model.

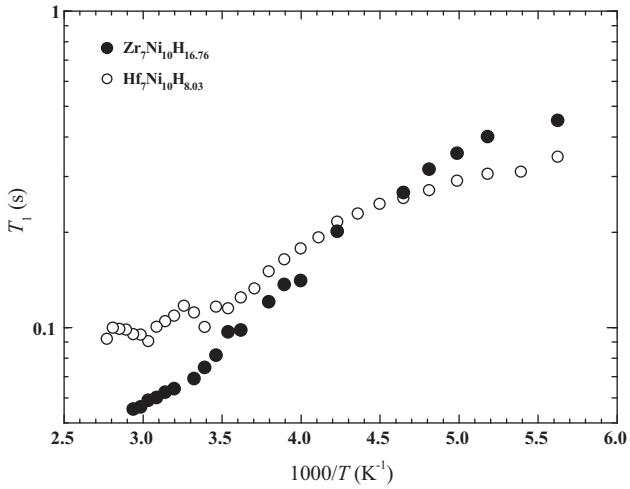

Fig. 4. Proton spin-lattice relaxation time T_1 at 20 MHz as a function of inverse temperature in $Zr_7Ni_{10}H_{16.76}$ and $Hf_7Ni_{10}H_{8.03}$.

the $Ti_{0.5}V_{1.9}Cr_{0.6}H_{5.03}$ (the lowest activation energy and shortest correlation time). The $TiV_{0.8}Cr_{1.2}H_{5.29}$ hydride is the last in the row.

3.2. $TiV_{0.8}Cr_{1.2}$ + 4 at.%Zr_7Ni_{10} and $TiV_{0.8}Cr_{1.2}$ + 4 at.%Hf_7Ni_{10} hydrides

Due to the rather low melting temperature of Zr_7Ni_{10} and Hf_7Ni_{10} additives, the final compositions of $TiV_{0.8}Cr_{1.2}$ + 4 at.%Zr_7Ni_{10} and $TiV_{0.8}Cr_{1.2}$ + 4 at.%Hf_7Ni_{10} consist of $TiV_{0.8}Cr_{1.2}$ crystallites covered by the additive as a shell. Zr_7Ni_{10} and Hf_7Ni_{10} exhibit rather fast hydrogen kinetics that helps to enhance the hydrogen sorption rate. To study the role of the additives in the intern hydrogen mobility we record the temperature dependence of proton T_1 in $TiV_{0.8}Cr_{1.2}$ + 4 at.%Zr_7Ni_{10} and $TiV_{0.8}Cr_{1.2}$ + 4 at.%Hf_7Ni_{10} composites. The magnetization recovery curves for ^{1}H T_1 in these composites are described by a single exponential decay over all temperature range.

In Fig. 3 we plot the ^{1}H T_1 values as a function of inverse temperature in pure $TiV_{0.8}Cr_{1.2}H_{5.03}$ hydride and with additives. It is seen that for composites the $T_1(1/T)$ curves become more asymmetric and the minimum is shifted towards the high temperature. Moreover, for the $TiV_{0.8}Cr_{1.2}$ + 4 at.%Zr_7Ni_{10} hydride the relaxation times T_1 at high temperature are slightly lower than in the pure hydride. In contrast to $TiV_{0.8}Cr_{1.2}$ + 4 at.%Zr_7Ni_{10}, in $TiV_{0.8}Cr_{1.2}$ + 4 at.%Hf_7Ni_{10} alloy the temperature dependence of T_1 is very similar to that one in the basic alloy $TiV_{0.8}Cr_{1.2}$, although the T_1 minimum is slightly shifted towards higher temperature.

To treat the experimental data we used the same model with almost the same parameters as for the basic alloy. The fitting parameters are also listed in Table 1. The main changes are following: increasing of the conduction electrons contribution (it affects more the low temperature region); increasing the relative contents of mobile hydrogen p_m; slight increasing the activation energy (the minimum of $T_1(1/T)$ is shifted towards the higher temperature). Because the activation energy E_a is mainly depended on the nearest neighbouring metallic atoms, it is possible that in the composites the main phase Ti–V–Cr has less vanadium. This assumption is in agreement with small decrease of the lattice parameters (see Table 1).

3.3. Zr_7Ni_{10} and Hf_7Ni_{10} hydrides

In Fig. 4 we present the temperature dependence of proton T_1 in $Zr_7Ni_{10}H_{16.76}$ and $Hf_7Ni_{10}H_{8.03}$ hydrides. It is clearly seen that in both hydrides T_1 decreases with temperature increase. Due to rather low desorption temperature we could not determine the T_1 (T) minima, which is obviously shifted towards higher temperatures. Nevertheless we can tell that $Zr_7Ni_{10}H_{16.76}$ is characterized by higher hydrogen mobility and rather wide activation energy distribution that is typical for amorphous alloys [18]. For $Hf_7Ni_{10}H_{8.03}$ two local minima is observed at T = 300 K and T = 360 K. More probably it is related to two different activation energy levels; however, for more accurate interpretation additional experimental data are required. And it is obvious that for these compounds one cannot neglect the relaxation due to paramagnetic Ni.

4. Conclusions

Proton spin-lattice relaxation measurements have shown:

- In Ti–V–Cr hydrides the relaxation strongly depends on the composition, namely the vanadium fraction; the activation process starts earlier in vanadium reach hydrides.
- The addition of Zr_7Ni_{10} or Hf_7Ni_{10} to $TiV_{0.8}Cr_{1.2}$ leads to increasing the relative contents of mobile hydrogen but simultaneously increases the activation energy. The last may be caused by the less vanadium fraction in the composites.
- $Zr_7Ni_{10}H_{16.76}$ is characterized by higher hydrogen mobility and rather wide activation energy distribution (compared to crystalline $Hf_7Ni_{10}H_{8.03}$) that is typical for amorphous alloys.

Acknowledgements

This work is partly granted by RFBR-CNRS, contract No. 07-08-92168 and developed under the IAEA project No 15933. We also grateful for a financial support of NoE INSIDEPORES (6th PCR-Europe) for stay of M.G.S. and N.E.S. at Institut Néel Grenoble.

References

[1] R.G. Barnes, in: H. Wipf (Ed.), Hydrogen in Metals III, Springer-Verlag, Berlin, Heidelberg, 1997, pp. 93–151.
[2] A.V. Skripov, Defect Diffus. Forum 224–225 (2003) 75–92.
[3] R. Hempelmann, A. Skripov, in: R.L. Schowen, et al. (Eds.), Hydrogen-Transfer Reaction, Wiley-VCH, Weinheim, 2007, pp. 787–829.

[4] G. Liang, J. Huot, S. Boily, A. Van Neste, R. Schulz, J. Alloys Compd. 292 (1999) 247–252.
[5] W. Oelerich, T. Klassen, R. Bormann, J. Alloys Compd. 315 (2001) 237–242.
[6] R.L. Corey, T.M. Ivancic, D.T. Shane, E.A. Carl, R.C. Bowman Jr., J.M. Bellosta von Colbe, M. Dornheim, R. Bormann, J. Huot, R. Zidan, A.C. Stowe, M.S. Conradi, J. Phys. Chem. C 112 (2008) 19784–19790.
[7] A.Ye. Yermakov, N.V. Mushnikov, M.A. Uimin, V.S. Gaviko, A.P. Tankeev, A.V. Skripov, A.V. Soloninin, A.L. Buzlukov, J. Alloys Compd. 425 (2006) 367–372.
[8] A.V. Skripov, A.V. Soloninin, A.L. Buzlukov, A.P. Tankeyev, A.Ye. Yermakov, N.V. Mushnikov, M.A. Uimin, V.S. Gaviko, J. Alloys Compd. 446–447 (2007) 489–494.
[9] M.S. Conradi, M.P. Mendenhall, T.M. Ivancic, E.A. Carl, C.D. Browning, P.H.L. Notten, W.P. Kalisvaart, P.C.M.M. Magusin, R.C. Bowman Jr., S.-J. Hwang, N.L. Adolphi, J. Alloys Compd. 446–447 (2007) 499–503.
[10] P.C.M.M. Magusin, W.P. Kalisvaart, P.H.L. Notten, R.A. van Santen, Chem. Phys. Lett. 456 (2008) 55–58.
[11] S. Miraglia, D. Fruchart, N. Skryabina, M. Shelyapina, B. Ouladiaf, E.K. Hlil, P. de Rango, J. Charbonnier, J. Alloys Compd. 442 (2007) 49–54.
[12] D. Fruchart, P. De Rango, J. Charbonnier, S. Miraglia, S. Rivoirard, N. Skryabina, Pulverulent intermetallic materials for the reversible storage of hydrogen, CNRS Patent 20100150822, 2010.
[13] H.T. Takeshita, N. Fujiwara, T. Oishi, D. Noréus, N. Takeichi, N. Kuriyama, J. Alloys Compd. 360 (2003) 250–255.
[14] N. Bloembergen, E.M. Purcell, R.V. Pound, Phys. Rev. 73 (1948) 679–712.
[15] V.I. Chizhik, V.S. Kasperovich, M.G. Shelyapina, Yu.S. Chernyshev, Int. J. Hydrogen Energy (2010), doi:10.1016/j.ijhydene.2010.10.082.
[16] T. Ueda, S. Hayashi, K. Hayamizu, Phys. Rev. B 48 (1993) 5837–5843.
[17] S. Hayashi, J. Solid State Chem. 170 (2003) 82–93.
[18] P.M. Richards, Phys. Rev. B 27 (1983) 2059–2072.